

Quantum nuclear effects on the location of hydrogen above and below the palladium (100) surface

Changjun Zhang, Angelos Michaelides*

London Centre for Nanotechnology and Department of Chemistry, University College London, London, WC1H 0AH, UK

ARTICLE INFO

Article history:

Received 12 October 2010

Accepted 4 January 2011

Available online 26 January 2011

Keywords:

Density functional calculation

Quantum effect

Path-integral

Palladium

Hydrogen

ABSTRACT

We report *ab initio* path integral molecular dynamics simulations of hydrogen and deuterium adsorbed on and absorbed in the Pd(100) surface at 100 K. Significant quantum nuclear effects are found by comparing with conventional *ab initio* molecular dynamics simulations with classical nuclei. For on-surface adsorption, hydrogen resides higher above the surface when quantum nuclear effects are included, an effect which brings the computed height into better agreement with experimental measurements. For sub-surface absorption, the classical and quantum simulations differ in an even more significant manner: the classically stable subsurface tetrahedral position is unstable when quantum nuclear effects are accounted for. This study provides insight that aids in the interpretation of experimental results and, more generally, underscores that despite the computational cost *ab initio* path integral molecular dynamics simulations of surface and subsurface adsorption are now feasible.

© 2011 Elsevier B.V. All rights reserved.

1. Introduction

The adsorption and absorption of hydrogen at palladium surfaces has great implications to a broad range of disciplines such as catalysis, nuclear materials, energy storage and superconductivity [1–3], to name a few. As a result a considerable body of work has been devoted to understanding at the atomic scale the adsorption and absorption of hydrogen at palladium surfaces [4–11]. It is generally accepted that palladium dissociates hydrogen molecules at its surfaces without appreciable activation energies, and that on-surface adsorption is favored over subsurface absorption which in turn is favored over bulk (interstitial site) absorption. Nonetheless, fundamental issues such as the adsorption and absorption positions are contentious, particularly the questions regarding how high above the surface or where below the surface the hydrogen atoms reside [12–17]. Despite the seeming simplicity of these questions, an accurate description of the specific hydrogen positions has proven challenging, not least because of the significant quantum nature of hydrogen atoms at surfaces (see e.g. ref. [18]).

Taking Pd(100) as an example, considerable experimental effort has been devoted to investigating the adsorption and absorption of hydrogen and its isotopes. Many studies [19–22], such as low energy electron diffraction (LEED) and electron energy loss spectroscopy (EELS), have found that hydrogen chemisorbs at the surface four-fold hollow site (4 F), as shown in Fig. 1; few however could provide direct

information on the height of hydrogen above the surface. By means of helium scattering, Rieder et al. [12] found that hydrogen adsorption at 110 K leads to the formation of a $p(1 \times 1)$ ordered phase at one monolayer (ML) coverage and a $c(2 \times 2)$ phase at 0.5 ML. They estimated that the normal distance from a hydrogen atom at the 4 F site to the topmost Pd layer (d_0) is ~ 0.35 Å and 0.65 – 0.70 Å for the $p(1 \times 1)$ and $c(2 \times 2)$ phases, respectively. By using a transmission channeling technique, Besenbacher et al. [13] found similar adsorption patterns for deuterium (D) at ~ 130 K, and they measured d_0 to be 0.3 ± 0.05 Å or 0.45 ± 0.15 Å for a $p(1 \times 1)$ phase or a $c(2 \times 2)$ phase, respectively.

Experiments have also suggested the existence of stable subsurface hydrogen atoms at low temperatures. The subsurface hydrogen atoms are believed to be more reactive than the surface hydrogen atoms, and thus have important implications in low temperature catalytic hydrogenation reactions [23–25]. In a series of experiments by Aruga et al. [26–29], mechanisms of H and D absorption were probed with temperature-programmed desorption and high-resolution EELS. Of particular interest is that below 120 K, the absorption coefficient is independent of temperature and quantum tunneling was suggested to be dominant in the process. It was also proposed that the absorbed atom lies at the tetrahedral (T_d) sites just beneath the surface (Fig. 1) with a ~ 1 ML coverage.

Whilst it can be difficult to determine the precise surface (and especially subsurface) hydrogen positions from experiments, *ab initio* calculations provide a useful tool in this regard. By using density functional theory (DFT), many authors [8,14,30] found that the subsurface T_d site is actually less favorable (by ~ 0.2 eV per H) than the subsurface octahedral (O_h) site where the H atom absorbs near

* Corresponding author.

E-mail address: angelos.michaelides@ucl.ac.uk (A. Michaelides).

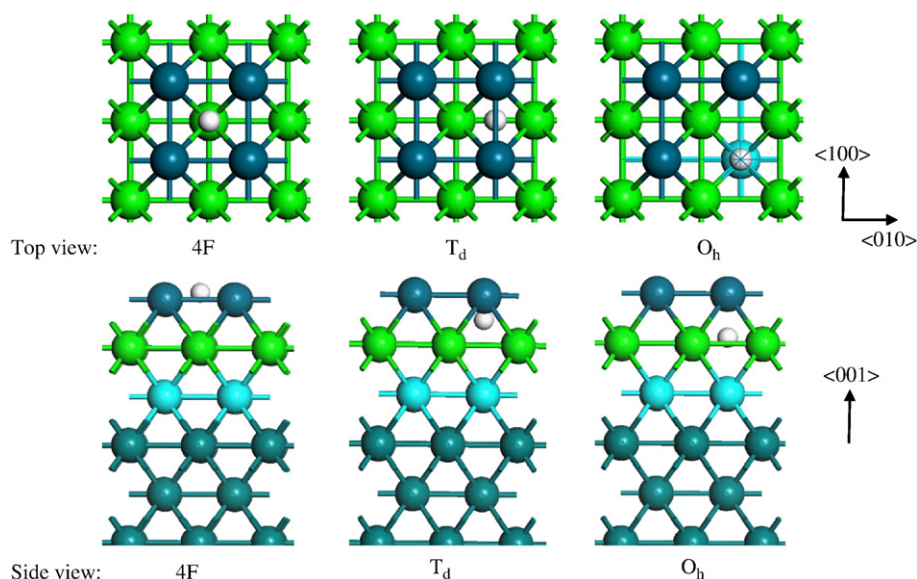


Fig. 1. Top and side views of a surface 4-fold hollow (4F) site, a subsurface tetrahedral (T_d) and a subsurface octahedral (O_h) site at the Pd(100) surface. H and Pd atoms are represented by white and colored balls, respectively. For the top view of the subsurface O_h site, the first-layer Pd atom, directly above the H atom, is shown as a small point for best viewing of the H atom.

the second Pd layer (Fig. 1). Hennig et al. [14], Tomanek et al. [15] and Hafner et al. [16,17] also used DFT to study hydrogen adsorption, predicting that at the 4F site the H atom is 0.24 Å, 0.11 Å and 0.20 Å above the surface, respectively, at 1.0 ML. However, because these are the results of standard total energy calculations, and neither finite temperature nor quantum nuclear effects are taken into account, caution must be exercised when comparing to experiments. Indeed, an important aspect and key general motivation for the current study is to examine the contribution from finite temperature and especially the quantum effects on the positions of both H and D in the system. To this end, we carry out both conventional *ab initio* molecular dynamics (AIMD) and *ab initio* path integral molecular dynamics (PIMD) simulations on H(D) adsorbed at and absorbed in the Pd(100) surface. In doing so, we determine the statistically averaged equilibrium positions. In particular, the PIMD approach [31,32], treats the nuclei as quantum particles and it provides a suitable method for exploring quantum nuclear effects on H(D) positions at finite temperatures. This study is also relevant to efforts to perform better and more realistic *ab initio* simulations. With the vast majority of DFT simulations being performed at the level of zero Kelvin geometry optimizations with classical nuclei (denoted as OPT hereafter), it can be difficult to establish if differences between experiment and theory are down to an intrinsic error of a given exchange correlation functional or to the absence of thermal and quantum effects. Thus the current study by tackling a well-defined experimental system may provide some insight that assists the detailed comparison between theory and experiment. Such studies are especially needed in solid state systems, where in contrast to the gas phase there is a relative paucity of accurate reference data.

The rest of the paper is organized as follows. In the next section, details of the calculations are outlined. The simulation results for hydrogen adsorption and absorption are presented in Subsections 3.1 and 3.2, respectively. In the former, we carry out a detailed comparison between the OPT, AIMD and PIMD results of the H(D) heights at the surface, and discuss the significant thermal and quantum effects observed. In the latter, instead of reporting the exact values for the positions, we show that the classical and quantum simulations differ in an even more significant manner: the classically stable subsurface tetrahedral position is unstable when quantum nuclear effects are accounted for. We discuss further in conjunction with experiments and conclude in the final Section 4.

2. Methodology

All calculations are carried out using the plane-wave pseudopotential DFT package, CASTEP [33]. Electron exchange and correlation is treated within the Perdew–Burke–Ernzerhof (PBE) generalized gradient approximation (GGA) [34], and the ionic cores are described by ultrasoft pseudopotentials [35]. The cutoff energy for the plane-wave expansion is set to be 400 eV, sufficiently high to give well-converged total energies and structures [36]. The maximum k-point spacing used is no greater than 0.02 \AA^{-1} , corresponding to a $12 \times 12 \times 1$ k-point mesh per (1×1) surface unit cell. With this setup, our calculations reproduce reasonably well the lattice constant (3.94 Å), bulk modulus (1.98 Mbar) and cohesive energy (3.83 eV) of Pd bulk, compared to the experiment data [37] (3.89 Å, 1.81 Mbar and 3.89 eV, respectively).

For the adsorption and absorption calculations we consider two unit cells, $p(1 \times 1)$ and $c(2 \times 2)$ of the Pd(100) surface, both of which were observed experimentally at low temperatures [12,13]. The slab used in the calculations has four Pd layers, with a vacuum region of around 11 Å along the surface normal. The bottom layer is kept at the bulk-truncated position whereas the remaining Pd layers and the H (D) atom are allowed to relax during the calculations. With this setup, the OPT calculations predict the height for a hydrogen atom adsorbed at the 4F site, d_0 , to be 0.129 Å at 1.0 ML. This value agrees with the 0.11–0.24 Å range obtained in previous DFT studies using various setups [14–17].

We have also carried out tests on the number of Pd layers used in the slab. Specifically, we find that when a seven-layer slab is used, d_0 is ~ 0.04 Å larger compared to the value obtained with the four-layer slab. In addition, we have also considered how possible expansion of the lattice induced by absorption may alter d_0 . To this end, we examined hydrogen on a Pd surface with a larger lattice constant corresponding to a PdH_{0.25} crystal (i.e. 25% H in Pd hydride). This test predicted a ~ 0.05 Å smaller value of d_0 than that obtained with the regular lattice constant. These differences are not particularly small. However, they are not critical in the present study, which aims primarily to explore the importance of thermal and quantum effects on the positions of hydrogen by examining the differences between OPT, AIMD and PIMD simulations. Indeed, this was confirmed with additional AIMD and PIMD tests on the seven-layer slab or the four-layer slab with the larger lattice constant, which showed that the magnitude of the thermal and quantum effects was not affected upon going from one slab to the other.

As opposed to OPT and standard DFT-based AIMD simulations, in which the nuclei are approximated as classical particles, the PIMD approach treats both electrons and atomic nuclei quantum mechanically. Very briefly, the PIMD method includes quantum effects on the nuclei in the framework of Feynman's path-integral formulation of quantum statistical mechanics [31,32]. The partition function of a many-body system can then be evaluated through a discretization of the density matrix along cyclic paths composed of a number of Trotter points (P). This means that each quantum degree of freedom is represented by a classical ring polymer consisting of P classical particles (termed beads) along the ring, connected by harmonic springs. To sample the configuration space of the classical isomorph of each quantum system, we use the molecular dynamics technique, as implemented by Probert and co-workers in CASTEP. Meanwhile, the many-body internuclear interactions can be obtained simultaneously from DFT calculations. The *ab initio* PIMD approach has successfully been applied to e.g. molecular [38], aqueous [39] and very recently surface systems [40].

Our PIMD calculations are carried out in the canonical ensemble at 100 K, close to the typical experimental temperatures used to study this system [12,13,17]. Both hydrogen and Pd nuclei are treated quantum mechanically. A Langevin thermostat is used to control the temperature and staging is employed to improve sampling efficiency [41]. The energy tolerance in the PIMD simulations is set to be 10^{-6} eV and the time-step for the dynamics is 0.5 fs. Because the path integral is discretized using P Trotter replicas, it is important to use a sufficient number of beads in the simulation to accurately capture the quantum nuclear effects of interest. Here, as in many other quantum studies [38–40], we choose $P=16$, a common choice given the extreme computational cost of *ab initio* PIMD simulations. Convergence tests with $P=32$ beads, which we now discuss, show that 16 beads is indeed a good compromise between accuracy and computational cost for the properties of interest in this adsorption system.

Of the various quantities produced in the PIMD simulations, we pay close attention in the convergence tests to the radius of gyration (RG) [42] and the height of the hydrogen isotopes above the surface. The radius of gyration along the surface normal (z), RG_z , is given by

$$\sqrt{\frac{1}{P} \left\langle \sum_{i=1}^P (r_z^i - \bar{r}_z)^2 \right\rangle},$$

where r_z^i and \bar{r}_z are the z coordinates of the hydrogen beads and the hydrogen centroid¹, respectively, and $\langle \dots \rangle$ indicates an ensemble average. RG_z describes the dispersion of the (D) nucleus along the surface normal, and thus is an important indicator of the extent of quantum nuclear delocalization. On the other hand, the height, d_0 , is directly relevant to the central question of this study. It is defined as the difference between the z coordinates of the hydrogen centroid and the centroid of the Pd atoms in the top layer (using the z coordinates of beads produces nearly identical averaged heights). Because of the thermal and quantum fluctuations of RG_z and d_0 , it is important to achieve well-converged results for these quantities. Taking the PIMD result of 1.0 ML H as an example, we illustrate in Fig. 2 how a well-converged ensemble-averaged value is achieved. After an initial equilibration for ~4 ps (not shown), we start the data collection, and monitor the instantaneous values and cumulative running averages of RG_z and d_0 . As can be seen, both quantities are quite stable for the ~18 ps shown. In particular, for the last 8 ps, the standard deviations of the cumulative averages are no more than 0.001 Å. We then choose the last 8 ps to calculate the mean value of the radius of gyration ($\overline{RG_z}$) and the height ($\overline{d_0}$). These mean values are also verified with a bootstrapping resampling method, which shows negligible difference. We find that the differences from using 16 beads and 32 beads are very small. The values of $\overline{RG_z}$ and $\overline{d_0}$ from using 32 beads is only 0.005 Å and 0.002 Å larger than those from using 16 beads. We shall see later that this difference does not affect our conclusions.

¹ The centroid of the quantum paths of a particle is defined as $\bar{r} = \frac{1}{P} \sum_{i=1}^P r_i$, r_i being the coordinates of the beads in the associated ring polymer.

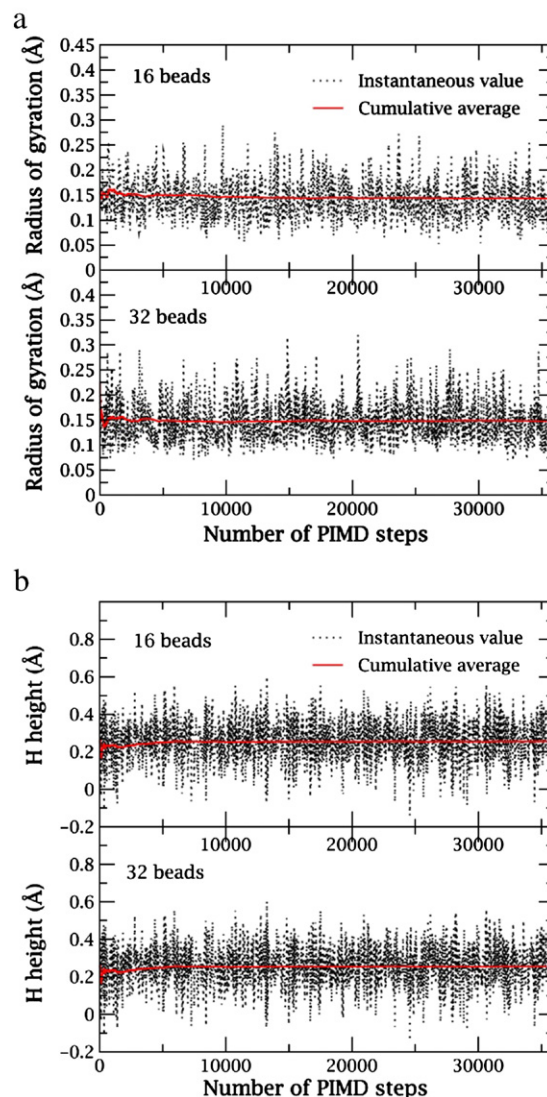


Fig. 2. At 1.0 ML coverage, (a) the radius of gyration for the nucleus along the surface normal (RG_z , defined in the text) from PIMD simulations using 16 and 32 beads; (b) the H height, which is the difference between the centroid coordinates of the H and first-layer Pd nuclei, calculated from PIMD simulations using 16 and 32 beads. In both (a) and (b), we start data collection after equilibrating the system for ~8000 steps (i.e. 4 ps, not shown), and we plot the instantaneous value (the black dotted line) and the cumulative running average (the red solid line).

3. Results and discussion

3.1. Adsorption at the surface

Fig. 3a shows the probability distribution of finding hydrogen at a certain height above the surface from the AIMD and PIMD simulations, along with the height predicted by the OPT calculation. Taking 1.0 ML H as an example, let us first compare the results from the OPT and AIMD simulations. The thermal effect is found to be significant, even though the temperature of the simulation is quite low. Whereas OPT predicts a H height of 0.129 Å, the distribution peak from the AIMD simulation appears at a noticeably higher position. The probability distribution has a reasonably large thermal broadening: the full width at half maximum (FWHM) for the height distribution, calculated from the standard deviation of the fluctuation, is 0.24 Å. Comparing now the results from AIMD and PIMD simulations, there is a noticeable shift towards higher height in the probability distribution in the latter, clearly indicative of

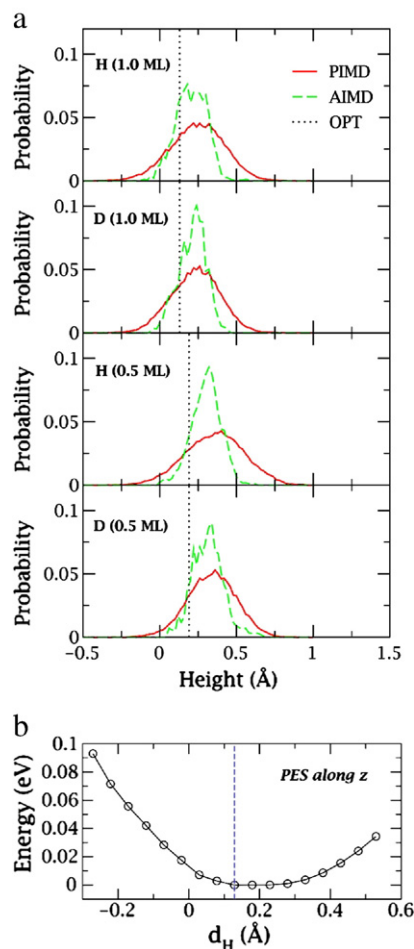


Fig. 3. (a) The probability distribution of finding hydrogen isotopes at a certain height above the surface from the *ab initio* molecular dynamics (AIMD) and *ab initio* path integral molecular dynamics (PIMD) simulations, along with the height predicted by the geometry optimization (OPT) calculation. (b) The potential well (PES, along the surface normal z) near the surface 4F site (in the 1×1 cell), represented as a function of the H height with respect to the 4F site (d_H). The minimum of the PES at 0.129 Å (i.e. the result from geometry optimization) is indicated by the dashed line.

the nuclear quantum effect. In addition, the FWHM for the PIMD result is 0.42 Å, indicating the large quantum fluctuation of the H nucleus. These differences between OPT, AIMD and PIMD can be also seen at 0.5 ML and for D at 1.0 ML and 0.5 ML.

Table 1

Heights (Å) of hydrogen isotopes above the surface and the percentage change (Δd_{12} , in %) in the first Pd interlayer spacing relative to the bulk interlayer spacing. In AIMD and PIMD, the averaged height (\bar{d}_0) is reported. The thermal and quantum fluctuations (Å) of the instantaneous height are represented by the standard deviation $\sigma_{d_0}^{\text{AIMD}}$ in AIMD and $\sigma_{d_0}^{\text{PIMD}}$ in PIMD, respectively. To describe the thermal and quantum fluctuations parallel to the surface, we also report the standard deviation of hydrogen along the $\langle 100 \rangle$ direction (see Fig. 1) in AIMD ($\sigma_{\langle 100 \rangle}^{\text{AIMD}}$) and PIMD ($\sigma_{\langle 100 \rangle}^{\text{PIMD}}$), respectively. The relevant experimental values are also included.

		1.0 ML		0.5 ML	
		H	D	H	D
Height	EXPT	~0.35 ^a	0.3 ± 0.05 ^b	0.65–0.70 ^a	0.45 ± 0.15 ^b
	OPT	0.129	0.129	0.190	0.190
	AIMD: \bar{d}_0 ($\sigma_{d_0}^{\text{AIMD}}$)	0.219 (0.101)	0.217 (0.096)	0.323 (0.101)	0.319 (0.096)
	PIMD: \bar{d}_0 ($\sigma_{d_0}^{\text{PIMD}}$)	0.253 (0.176)	0.243 (0.156)	0.365 (0.191)	0.346 (0.159)
Fluctuation along $\langle 100 \rangle$	AIMD: $\sigma_{\langle 100 \rangle}^{\text{AIMD}}$	0.056	0.047	0.037	0.034
	PIMD: $\sigma_{\langle 100 \rangle}^{\text{PIMD}}$	0.172	0.156	0.188	0.152
	First Pd layer spacing (Δd_{12})	EXPT	+2.5–5.8 ^c	–	–
	OPT	+4.27	+4.27	+1.93	+1.93
	AIMD	+4.83	+4.84	+1.99	+2.13
	PIMD	+4.89	+4.68	+2.10	+2.07

^a Ref. [12].

^b Ref. [13].

^c Ref. [44].

To get a clearer picture of the height, we summarize in Table 1 the values of \bar{d}_0 , the calculations and accuracy tests of which are described in Section 2. The error bar of less than 0.001 Å in \bar{d}_0 gives us confidence to make comparison between the AIMD and PIMD calculations. We also report the thermal and quantum fluctuations of d_0 , which are characterized by the standard deviation of d_0 in AIMD ($\sigma_{d_0}^{\text{AIMD}}$) and the standard deviation of d_0 in PIMD ($\sigma_{d_0}^{\text{PIMD}}$). Of course, thermal effects will also be present in the finite temperature PIMD simulation, and thus differences between $\sigma_{d_0}^{\text{PIMD}}$ and $\sigma_{d_0}^{\text{AIMD}}$ provide an estimate of the pure quantum contributions.

From Table 1, thermal and quantum effects can be clearly seen. First, by comparing the AIMD to the OPT results, the thermal effect is large, suggested by the ~0.1 Å difference between them. Second, by examining the differences of \bar{d}_0 from the AIMD and PIMD simulations, the quantum effect on the height is small but significant, being on the order of 0.04 Å for H and 0.03 Å for D. Isotopic effects also emerge from the PIMD results: the differences between the values of \bar{d}_0 obtained for H and D in the PIMD simulations is noticeably larger than those obtained from the AIMD simulations.

It is interesting to note that both PIMD and AIMD predict a higher position than OPT does, and PIMD also predicts a higher position than AIMD does. Both effects are likely a consequence of the asymmetric potential well the hydrogen isotopes experience along the surface normal. To illustrate this, we plot the potential for a hydrogen atom in a range along the surface normal that is slightly above and below the surface. As shown in Fig. 3b, the potential to move hydrogen away from the surface (i.e. $d_0 > 0.129$ Å, the OPT minimum indicated by the dashed line) is shallower than the potential to push hydrogen towards the surface ($d_0 < 0.129$ Å). This is the standard asymmetric bonding potential that leads to thermal expansion in materials and in this system to the H residing further from the surface. Specifically, in the AIMD simulations, thermal fluctuations allow the particle to distribute more on the shallower side of the potential with the consequence that the particle ends up at a position higher than that predicted in the geometry optimization; In PIMD, the quantum fluctuations enable the beads representing the particle to populate the shallower side of the potential well, and thus the particle resides even higher above the surface.

Before moving on to consider subsurface hydrogen, we briefly address several other aspects of the chemisorbed hydrogen system. First, in both AIMD and PIMD, the distribution of H or D is centralized at the 4F site, and there is no diffusion to neighboring 4F sites throughout the simulations. Second, although hydrogen remains localized at the 4F site, pronounced quantum fluctuations are also observed for the adsorbed hydrogen within the surface plane (i.e. parallel to the surface). To quantify this, we report in Table 1 the standard deviations of the

coordinates along $\langle 100 \rangle$ direction (Fig. 1) in AIMD and PIMD simulations, denoted as $\sigma_{\langle 100 \rangle}^{\text{AIMD}}$ and $\sigma_{\langle 100 \rangle}^{\text{PIMD}}$, respectively. Differences between the two quantities can be clearly seen. Results obtained from the coordinates along $\langle 010 \rangle$ direction are nearly identical to those along $\langle 100 \rangle$ direction and thus are omitted. Third, it has been shown before that the quantum delocalization of hydrogen can also have an indirect impact on the heavier atoms to which the hydrogens are bonded [38,40]. Therefore, we considered the influence, if any, the quantum hydrogen has on the Pd atoms, by specifically examining the interlayer spacing between the top two Pd layers (d_{12})². As reported in Table 1, all theories predict an expansion of d_{12} , as expected. However, there is very little difference between the AIMD and PIMD results, suggesting negligible quantum effects on Pd.

3.2. Absorption into the surface

When a H atom absorbs into the surface, the subsurface T_d and O_h sites are the two possible stable sites to accommodate it, as found here and in previous calculations [16,30]. For absorption near the subsurface O_h site, the H is 0.37 Å above the second Pd layer in the (1×1) cell, which agrees with the previous OPT result (0.39 Å) in the same cell [16]. For absorption near the subsurface T_d site, our calculations predict a position which is 1.16 Å above the second Pd layer and 1.11 Å below the first Pd layer in the (1×1) cell (no corresponding experimental or theoretical data has been found). Questions however are how different the absorption at these sites could be when thermal and quantum effects are included. Before presenting the AIMD and PIMD results, it is useful to examine the DFT total energy profile for the absorption process. For illustration purposes, we show the results obtained from the (1×1) cell in Fig. 4, where the binding energy relative to a gas phase hydrogen molecule is indicated for surface and subsurface hydrogen and the transition states that connect some of the sites considered. Note that we have tested with the seven-layer model and found similar results. In particular, the difference between energy barriers from the four-layer and seven-layer models is less than 0.01 eV. As with previous studies [16,30], our calculations show that on-surface adsorption is favorable to subsurface absorption, and the subsurface O_h site is preferred over the T_d site. In addition, we also find that the energy barrier³ for a H atom at the subsurface T_d site to diffuse to the 4F site is quite small (~ 0.05 eV), implying that the resurfacing process can be facile.

We have also considered the effects from the zero-point energies (ZPE), based on the harmonic approximation, which is the simplest way to account for quantum effects. Specifically, we plot in Fig. 4 the ZPE-corrected binding energy in which ZPE for the adsorbed (or adsorbed) hydrogen isotopes and the gas phase H_2 or D_2 molecule are all included. As can be seen, ZPE stabilizes hydrogen adsorption at the 4F site by ~ 0.05 , and conversely, ZPE destabilizes hydrogen adsorption at the subsurface T_d site by ~ 0.05 eV. The resurfacing barrier from the subsurface T_d site becomes negligible. Similar ZPE effects are also seen in the case of deuterium. These results are very interesting, as they imply that if the quantum effect is significant enough, the already small classical barriers could be washed out so as to alter the resurfacing or absorption mechanism. Indeed, as we now discuss, this was found to be the case in our PIMD simulations.

As shown in Fig. 5, starting with a hydrogen atom at the subsurface T_d site at 1.0 ML, the potential energy from the PIMD simulation remains flat for the first ~ 1 ps, then it fluctuates drastically in the next ~ 1 ps until the energy finally settles at a new lower value. This energy evolution

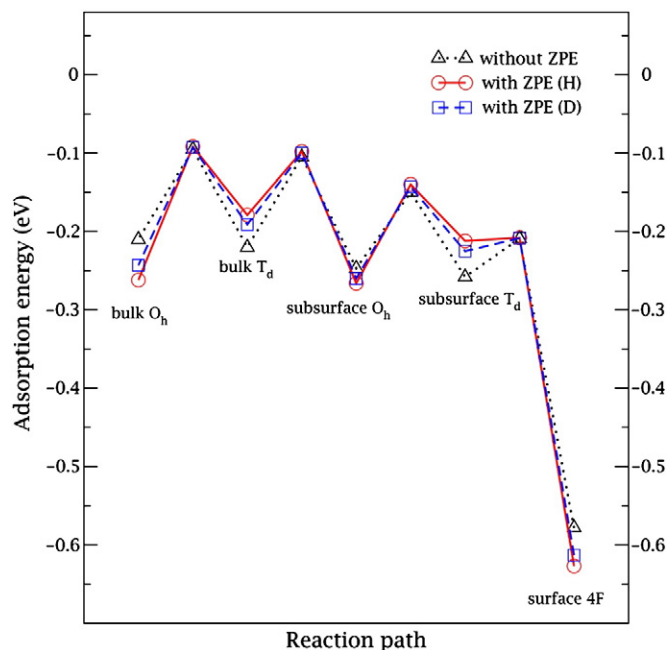


Fig. 4. Variations of adsorption energy at zero Kelvin along the absorption (or resurfacing) path calculated in the (1×1) cell. The adsorption energy is calculated by subtracting the half total energy of the gas phase H_2 molecule and the total energy of the bare surface from the total energy of a specific adsorption state. The energy minima represent adsorption at various sites, and the maxima represent the transition states. The zero-point corrected adsorption energies (ZPE) are also plotted.

clearly indicates a transition from absorption at the initial T_d site to a new site with a lower energy, which is found to be the surface 4F site in this case. In the conventional AIMD simulation, on the other hand, the potential energy remains constant throughout the 40 ps run, and no change in absorption site is observed. This fundamental difference between the classical and quantum simulations is observed not only for H at 1.0 ML, but also for H at 0.5 ML and for D at both 0.5 and 1.0 ML. Thus, it appears that when quantum nuclear effects are accounted for the subsurface T_d site is not a stable adsorption site at finite temperature. To further test this conclusion, we repeat the AIMD and PIMD simulations for a H atom adsorbed in two Pd surfaces which are modeled with seven layers of Pd and with an expanded lattice constant (as described in Section 2) respectively. In both cases, the H atom at the subsurface T_d site is again found to be unstable and within 2 ps in the

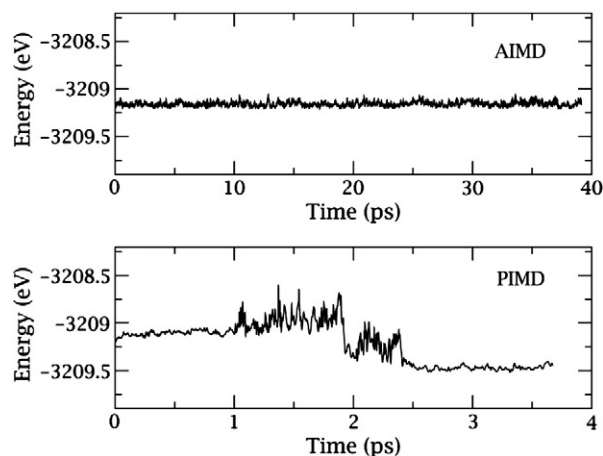


Fig. 5. Starting with a H atom at the subsurface T_d site, the potential energy evolutions in the AIMD and PIMD simulations at 1.0 ML. In the AIMD simulation, the H atom remains in the T_d site and the potential energy remains flat throughout the entire 40 ps. In contrast, in the PIMD simulation, the H atom leaves the T_d site after only ~ 1 ps. Similar behavior is also observed for H at 0.5 ML and for D at 0.5 and 1.0 ML.

² It is also known that d_{12} exhibits an anomalous expansion relative to the bulk ($\Delta d_{12} = +2.5\% \sim +4.6\%$) in experiments (Behm, R. J. et al. *Surf. Sci. Lett.* **1979**, 88, L59; Burchhardt, J. et al. *Surf. Rev. Lett.* **1996**, 3, 1339). As a plausible way to reconcile the discrepancy, hydrogen contamination was proposed: H interacts with the surface, weakening the Pd–Pd bonds, and thereby expanding d_{12} (Kim et al. *Phys. Rev. B* **2005**, 71, 205418; Quinn, J. et al. *Phys. Rev. B* **1990**, 42, 11348).

³ The energy barrier was calculated using a combined linear and quadratic synchronous transit method implemented in the CASTEP code.

PIMD simulations it moves to the 4F site, whereas it stays at the T_d site in the AIMD simulations. For a H or D atom initially adsorbed at the subsurface O_h site, our PIMD simulations show that there is no jumping or transformation to a different absorption site. However, because of the heavy computational cost, we did not strive to obtain a well-converged position at the O_h site, as we did for the more stable 4 F site.

4. Conclusions

From the PIMD simulations, we see clearly that quantum nuclear effects have a strong impact on both the adsorption and absorption of H and D. In some cases, even fundamental differences are observed between quantum and classical simulations. For the on-surface adsorption, the PIMD simulations predict the hydrogen isotopes to reside significantly higher than those by the classical simulations, and move the results in the right direction towards experiment. Moreover, the PIMD simulations distinguish the heights of the hydrogen isotopes, which again agrees with the experimental findings. These results strongly suggest that to narrow the gap between experiment and theory, a finite temperature quantum approach such as PIMD is very useful.

For the subsurface absorption, the PIMD simulations reveal a fundamentally different result from the classical simulations. The fact that the subsurface T_d site is unstable in PIMD provides some new insight into the absorption and resurfacing processes. Apparently, we can re-interpret the experiments of Aruga et al. [26] who assigned the adsorbed H atom to subsurface T_d sites. That is to say, the observed ~1 ML H (or D) should be at the subsurface O_h sites. Moreover, the long-held classical absorption or resurfacing path [43,44], involving, in sequence, a 4F site, a trigonal site (i.e. a transition state or the maximum point in Fig. 5), a subsurface T_d site, another trigonal site and a subsurface O_h site, is not the actual route. Since the washing out of the classical barrier, the absorption or resurfacing process could occur without going through the unstable subsurface T_d site, and the process should also become more facile than that predicted by the classical theory.

Acknowledgements

This work is supported by the E.P.S.R.C. and the European Research Council. A. M. is also supported by the EURYI scheme (See www.esf.org/euryi). We are grateful to the LCN and UCL Research Computing for computational resources. We are also grateful to the Materials Chemistry Consortium for access to the HECToR and HPCx facilities (EPSRC grant EP/F067496). Discussions within the ICE group at LCN are also warmly acknowledged.

References

- [1] B. Stritzker, W. Buckel, *Z. Phys.* 257 (1972) 1.
- [2] B. Bennemann, W. Buckel, *Z. Phys.* 260 (1973) 367.
- [3] F.A. Lewis, *Int. J. Hydrogen Energy* 6 (1981) 319.
- [4] R.J. Behm, K. Christmann, G. Ertl, *Surf. Sci.* 99 (1980) 320.
- [5] C. Nyberg, C.G. Tengstal, *Phys. Rev. Lett.* 50 (1983) 1680.
- [6] K. Christmann, *Surf. Sci. Rep.* 9 (1988) 1.
- [7] W.A. Oates, A.M. Stoneham, *J. Phys. F* 13 (1983) 2427.
- [8] L.L. Jewell, B.H. Davis, *Appl. Catal.*, A 310 (2006) 1.
- [9] A. Michaelides, Z. Liu, C. Zhang, A. Alavi, D.A. King, P. Hu, *J. Am. Chem. Soc.* 125 (2003) 3704.
- [10] M. Wilde, K. Fukutani, *Phys. Rev. B* 78 (2008) 115411.
- [11] A. Gross, *Chemphyschem* 11 (2010) 1374.
- [12] K.H. Rieder, W. Stocker, *Surf. Sci.* 148 (1984) 139.
- [13] F. Besenbacher, I. Stensgaard, K. Mortensen, *Surf. Sci.* 191 (1987) 288.
- [14] D. Hennig, S. Wilke, R. Lober, M. Methfessel, *Surf. Sci.* 287 (1993) 89.
- [15] D. Tomanek, Z. Sun, S.G. Louie, *Phys. Rev. B* 43 (1991) 4699.
- [16] W. Dong, V. Ledentu, P. Sautet, A. Eicher, J. Hafner, *Surf. Sci.* 411 (1998) 123.
- [17] A. Eicher, J. Hafner, G. Kresse, *J. Phys. Condens. Matter* 8 (1996) 7659.
- [18] M. Nishijima, H. Okuyama, N. Takagi, T. Aruga, W. Brenig, *Surf. Sci. Rep.* 57 (2005) 113.
- [19] R.J. Behm, V. Penka, M.G. Cattania, K. Christmann, G.J. Ertl, *Chem. Phys.* 78 (1983) 7486.
- [20] C. Nyberg, C.G. Tengstal, *Surf. Sci.* 126 (1983) 163.
- [21] W. Eberhardt, F. Greuter, E.W. Plummer, *Phys. Rev. Lett.* 46 (1981) 1085.
- [22] T.E. Felter, S.M. Foiles, M.S. Daw, R.H. Stulen, *Surf. Sci.* 171 (1986) L379.
- [23] A.D. Johnson, S.P. Daley, A.L. Utz, S.T. Ceyer, *Science* 257 (1992) 223.
- [24] A. Michaelides, P. Hu, A. Alavi, *J. Chem. Phys.* 111 (1999) 1343.
- [25] S. Wright, J.F. Skelly, A. Hodgson, *Chem. Phys. Lett.* 364 (2002) 522.
- [26] H. Okuyama, T. Nakagawa, W. Siga, N. Takagi, M. Nishijima, T. Aruga, *Surf. Sci.* 411 (1998) L849.
- [27] H. Okuyama, W. Siga, N. Takagi, M. Nishijima, T. Aruga, *Surf. Sci.* 401 (1998) 344.
- [28] M. Wilde, M. Matsumoto, K. Fukutani, T. Aruga, *Surf. Sci.* 482 (2001) 346.
- [29] H. Okuyama, T. Nakagawa, W. Siga, N. Takagi, M. Nishijima, T. Aruga, *J. Phys. Chem. B* 103 (1999) 7876.
- [30] S. Wilke, D. Hennig, R. Lober, M. Methfessel, M. Scheffler, *Surf. Sci.* 307 (1994) 76.
- [31] R.P. Feynman, A.R. Hibbs, *Quantum Mechanics and Path Integrals*, McGraw-Hill, 1965.
- [32] D. Marx, M. Parrinello, *J. Chem. Phys.* 104 (1996) 4077; D. Marx, M. Parrinello, *Z. Phys. B* 95 (1994) 143; M.E. Tuckerman, D. Marx, M.L. Klein, M. Parrinello, *J. Chem. Phys.* 104 (1996) 5579.
- [33] S.J. Clark, M.D. Segall, C.J. Pickard, P.J. Hasnip, M.I.J. Probert, K. Refson, M.C. Payne, *Z. fuer Kristallographie* 567 (2005) 220.
- [34] J.P. Perdew, K. Burke, M. Ernzerhof, *Phys. Rev. Lett.* 77 (1996) 3865.
- [35] D. Vanderbilt, *Phys. Rev. B* 41 (1990) 7892.
- [36] C. Zhang, A. Alavi, *J. Am. Chem. Soc.* 127 (2005) 9808.
- [37] C. Kittel, *Introduction to Solid State Physics*, 7th ed., John Wiley & Sons, Inc., 1996.
- [38] M.E. Tuckerman, D. Marx, *Phys. Rev. Lett.* 86 (2001) 4946.
- [39] M.E. Tuckerman, D. Marx, M. Parrinello, *Nature* 417 (2002) 925.
- [40] X.Z. Li, M.I.J. Probert, A. Alavi, A. Michaelides, *Phys. Rev. Lett.* 104 (2010) 066102.
- [41] M.E. Tuckerman, D. Marx, M.L. Klein, M. Parrinello, *J. Chem. Phys.* 104 (1996) 5579.
- [42] M.J. Gillan, *Philos. Mag. A* 58 (1988) 257.
- [43] P. Kamakoti, D.S.J. Sholl, *Membr. Sci.* 225 (2003) 145.
- [44] S.Z. Baykara, *Int. J. Hydrogen Energy* 29 (2004) 1631.